Scientific Journal Impact Factor (SJIF): 5.278
International Journal of Modern Trends in Engineering and Research
IJMTER
ISSN (ONLINE) : 2349 - 9745
ISSN (PRINT) : 2393 - 8161

MODELING AND SIMULATION OF THREE PHASE INDUCTION MOTOR ELECTRICAL FAULTS USING MATLAB/SIMULINK

Reuben, J[1], Onah, C. O[2] and J. U. Agber[3]
[1,2,3]*Department of Electrical and Electronics Engineering, University of Agriculture, Makurdi, Nigeria*

Abstract— Induction motors are the most widely used motors due to their reliability, robustness, low cost, easy operation, high efficiency and having simple control gear for starting and speed control. The usefulness of this motor has given rise to a lot of studies including the transient behavior of the machine. This paper presents detailed modeling of an induction machine using dq0 axis transformations of the stator and rotor variables into arbitrary reference frame because of the highly coupled nature of the machine, especially the inductances within the windings. While other methodologies are feasible with MATLAB/Simulink, an embedded MATLAB toolbox is utilized in this paper due to its uniqueness in offering the user the opportunity of programming the differential equations rather than obtaining the complete block diagram representation of those equations. Equations in the natural reference frame, derivation of machine inductances, transformation of stator and rotor variables to arbitrary reference frame, as well as torque equations are presented. The model is used to ascertain the effects of electrical fault conditions such as unbalanced voltage, single phasing, over load, phase reversal and under voltage conditions on the dynamic performance of the motor. The proposed model has been developed and simulated using MATLAB/Simulink and the results are similar to those obtained elsewhere [1]-[3].

Keywords— Arbitrary reference frame, dq0 axis transformation, Electrical faults, Induction Motor (IM), MATLAB/Simulink.

I. INTRODUCTION

Electrical Machinery is more than 100 years old. While new types of machines have emerged recently, bulk of the electrical energy conversion systems is still dominated by classical induction machines (motors and transformers). The productivity of the industrial systems based on these drives is very critical. While reliability of this operation is of paramount importance, it is frequently impaired by faults. The study of performance of these machines under fault conditions gives better idea of their performance, which may assist engineers in making their choice while designing. The induction motors are by far the most used electro-mechanical device in industry today due to the advantages they have over other types of motors. They are cheap, rugged, easily maintainable and can be used in hazardous locations [1], [4]-[6]. However, induction motors are susceptible to many types of electrical faults such as over voltage, over current, overload, temperature rise, single phasing, phase reversal, voltage unbalanced and under voltage in industrial applications.

A motor fault that is not identified early may become catastrophic, leading to severe damage. These faults in three phase induction machines heat both stator and rotor windings and if undetected may cascade into motor failure, which in turn may cause production shutdown. Such industrial shutdowns are costly in terms of lost production time, maintenance costs and wasted raw materials. Even though faults on induction motor can be either mechanical or electrical faults [7]-[9], electrical faults are usually influenced by power quality that is supplied by ac grid, such as variations of frequency and unbalanced voltage.

This paper models the common electrical faults such as voltage unbalanced, over voltage, under voltage, single phasing, phase reversal and overload that occur in three phase induction motor and analyses their effects on the operation of the motor. The MATLAB/Simulink approach is used in this paper for solving the differential equations rather than obtaining their block diagram representation. Modeling of three-phase induction motor using Park's Transformation is hereby presented.

II. MODELING OF THREE PHASE INDUCTION MOTOR

The winding arrangement of a symmetrical induction machine is shown in Figure 1. The stator windings are identical and sinusoidally distributed, displaced 120˚ apart, with equivalent turns N_s and resistance r_s per winding per phase. Similarly, the rotor windings are also considered as three identical sinusoidally distributed windings, displaced 120˚ apart, with equivalent turns N_r and resistance r_r per winding per phase.

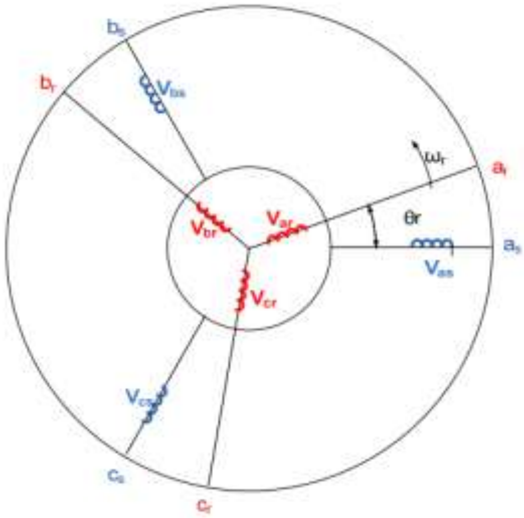

Figure 1. Three Phase Winding Arrangement

A. Voltage equations

Using Kirchhoff's Voltage Law, the voltage equations for each winding on the stator and rotor can be determined.

Stator Windings:

$$V_{as} = r_s I_{as} + \frac{d\lambda_{as}}{dt} \tag{1}$$

$$V_{bs} = r_s I_{bs} + \frac{d\lambda_{bs}}{dt} \tag{2}$$

$$V_{cs} = r_s I_{cs} + \frac{d\lambda_{cs}}{dt} \tag{3}$$

Rotor Windings:

$$V_{ar} = r_r I_{ar} + \frac{d\lambda_{ar}}{dt} \tag{4}$$

$$V_{br} = r_r I_{br} + \frac{d\lambda_{br}}{dt} \tag{5}$$

$$V_{cr} = r_r I_{cr} + \frac{d\lambda_{cr}}{dt} \tag{6}$$

The subscript 'a', 'b', 'c' refer to the phases, 's', 'r' refer to stator and rotor variables, while 'V', 'I', and 'λ' referring to instantaneous voltage, current and flux linkage respectively.

It is very convenient to first refer all rotor variables to the stator by applying the appropriate turns ratio. Equations (7)-(9) represents all rotor variables and is expressed in a simplified way including the variables of all the rotor phases in one equation.

$$I'_{abcr} = \frac{N_r}{N_s} I_{abcr} \tag{7}$$

$$V'_{abcr} = \frac{N_r}{N_s} V_{abcr} \tag{8}$$

Volume: 5, Issue: 05, [May– 2018] ISSN (Online):2349–9745 ; ISSN (Print):2393-8161

$$\lambda'_{abcr} = \frac{N_r}{N_s}\lambda_{abcr} \tag{9}$$

B. Inductances

The flux linkages as seen in equations (1)-(6) are functions of inductance and therefore the inductances within the motor must be determined. The inductances within the motor consist of self-inductance, leakage inductance, magnetizing inductance and mutual inductance. The flux linkage equation is shown in equation (10) and contains the inductance matrix [L].

$$\begin{bmatrix}\lambda_{as}\\ \lambda_{bs}\\ \lambda_{cs}\\ \lambda_{ar}\\ \lambda_{br}\\ \lambda_{cr}\end{bmatrix} = \begin{bmatrix} L_{asas} & L_{asbs} & L_{ascs} & L_{asar} & L_{asbr} & L_{ascr}\\ L_{bsas} & L_{bsbs} & L_{bscs} & L_{bsar} & L_{bsbr} & L_{bscr}\\ L_{csas} & L_{csbs} & L_{cscs} & L_{csar} & L_{csbr} & L_{cscr}\\ L_{aras} & L_{arbs} & L_{arcs} & L_{arar} & L_{arbr} & L_{arcr}\\ L_{bras} & L_{brbs} & L_{brcs} & L_{brar} & L_{brbr} & L_{brcr}\\ L_{cras} & L_{crbs} & L_{crcs} & L_{crar} & L_{crbr} & L_{crcr}\end{bmatrix} \times \begin{bmatrix}I_{as}\\ I_{bs}\\ I_{cs}\\ I_{ar}\\ I_{br}\\ I_{cr}\end{bmatrix} \tag{10}$$

where the inductance is defined by the subscript, L_{asas} refers to the inductance between winding as and winding as, meaning self-inductance in winding as; and L_{asbr} refers to the inductance between winding as and winding br, meaning mutual inductance.

The self-inductance in the stator windings consists of magnetizing and leakage inductances. The windings are identical and therefore the self-inductance of all the stator windings will be identical.

$$L_{asas} = L_{bsbs} = L_{cscs} = L_{ms} + L_{ls} \tag{11}$$

The magnetizing inductance (L_{ms}) can be expressed as in equation (12) [10].

$$L_{ms} = \frac{\mu_o \ell r N_s^2 \pi}{4g} \tag{12}$$

The self-inductance in the rotor windings is similar to that of the stator windings.

$$L_{arar} = L_{brbr} = L_{crcr} = L_{mr} + L_{lr} \tag{13}$$

With the magnetizing inductance expressed as in equation (14) [10]

$$L_{mr} = \frac{\mu_o \ell r N_r^2 \pi}{4g} \tag{14}$$

Where N_s and N_r are the effective number of turns of the stator and rotor windings, r is the radius of the motor cross-section, ℓ is the length of the motor cross-section and g is the air-gap radial length.

Stator-stator mutual inductance can be expressed as equation (15) [10].

$$L_{xsys} = \frac{\mu_o \ell r N_s^2 \pi}{4g} \cos\theta_{xsys} \tag{15}$$

Where L_{xsys} and θ_{xsys} are the inductance and angle between any stator winding 'x' and any other stator winding 'y'.

Using equation (12), equation (15) can be modified to be:

$$L_{xsys} = L_{ms}\cos\theta_{xsys} \tag{16}$$

Considering the winding distribution in Figure 1, it can be seen that the only possible displacement between two stator windings are 120^o and 240^o in both directions. This implies that $\cos\theta_{xsys}$ in equation (16) can be evaluated as follows:

$$\cos\theta_{xsys} = \cos(\pm 120^o) = \cos(\pm 240^o) = -\frac{1}{2} \tag{17}$$

From equations (16) and (17) the expression describing the mutual inductance between any two stator windings can be simplified to equation (18).

$$L_{asbs} = L_{ascs} = L_{bscs} = L_{bsas} = L_{csas} = L_{csbs} = -\frac{1}{2}L_{ms} \tag{18}$$

The rotor-rotor mutual inductances are similar to that of the stator-stator mutual inductances and can be expressed as:

$$L_{arbr} = L_{arcr} = L_{brcr} = L_{brar} = L_{crar} = L_{crbr} = -\frac{1}{2}L_{mr}$$

Volume: 5, Issue: 05, [May– 2018] ISSN (Online):2349–9745 ; ISSN (Print):2393-8161

The stator-rotor mutual inductances depend on the position of the rotor according to the following relationship [11].

$$L_{xsyr} = L_{sr} \cos \theta_{xsyr} \quad (19)$$

where L_{xsyr} is the mutual inductance between any stator winding 'x' and any rotor winding 'y'; and θ_{xsyr} is the angle between them.

The expression for L_{sr} in equation (19) is given by equation (20).

$$L_{sr} = \left(\frac{N_s}{2}\right)\left(\frac{N_r}{2}\right)\frac{\mu_o \pi r \ell}{g} \quad (20)$$

The expression for the stator-rotor mutual inductances can be deduced using equation (19) and Figure 1.

$$L_{asar} = L_{bsbr} = L_{cscr} = L_{sr} \cos \theta_r \quad (21)$$

$$L_{asbr} = L_{bscr} = L_{csar} = L_{sr} \cos\left(\theta_r + \frac{2\pi}{3}\right) \quad (22)$$

$$L_{ascr} = L_{bsar} = L_{csbr} = L_{sr} \cos\left(\theta_r - \frac{2\pi}{3}\right) \quad (23)$$

Likewise, rotor-stator mutual inductances are:

$$L_{aras} = L_{brbs} = L_{crcs} = L_{sr} \cos(-\theta_r) \quad (24)$$

$$L_{arbs} = L_{brcs} = L_{cras} = L_{sr} \cos\left(\frac{2\pi}{3} - \theta_r\right) \quad (25)$$

$$L_{arcs} = L_{bras} = L_{crbs} = L_{sr} \cos\left(\frac{4\pi}{3} - \theta_r\right) \quad (26)$$

The inductance matrix equation (10) is divided into four sub-matrices.

$$L = \begin{bmatrix} L_s & L_{SR} \\ L_{RS} & L_r \end{bmatrix} \quad (27)$$

Where L_s is the inductance within the stator windings, L_r is the inductances within the rotor windings, L_{SR} is the inductances between stator and rotor windings and L_{RS} is the inductances between the rotor and stator windings.

Using the inductances in equation (10) as divided in equation (27) and substituting derived inductances yield the following:

$$L_s = \begin{bmatrix} L_{ms} + L_{ls} & -\frac{1}{2}L_{ms} & -\frac{1}{2}L_{ms} \\ -\frac{1}{2}L_{ms} & L_{ms} + L_{ls} & -\frac{1}{2}L_{ms} \\ -\frac{1}{2}L_{ms} & -\frac{1}{2}L_{ms} & L_{ms} + L_{ls} \end{bmatrix} \quad (28)$$

$$L'_{SR} = L_{ms} \begin{bmatrix} \cos \theta_r & \cos\left(\theta_r + \frac{2\pi}{3}\right) & \cos\left(\theta_r - \frac{2\pi}{3}\right) \\ \cos\left(\theta_r - \frac{2\pi}{3}\right) & \cos \theta_r & \cos\left(\theta_r + \frac{2\pi}{3}\right) \\ \cos\left(\theta_r + \frac{2\pi}{3}\right) & \cos\left(\theta_r - \frac{2\pi}{3}\right) & \cos \theta_r \end{bmatrix} \quad (29)$$

$$L'_r = \begin{bmatrix} L'_{lr} + L_{ms} & -\frac{1}{2}L_{ms} & -\frac{1}{2}L_{ms} \\ -\frac{1}{2}L_{ms} & L'_{lr} + L_{ms} & -\frac{1}{2}L_{ms} \\ -\frac{1}{2}L_{ms} & -\frac{1}{2}L_{ms} & L'_{lr} + L_{ms} \end{bmatrix} \quad (30)$$

Equations (29) and (30) are the mutual inductances and inductances within the rotor windings referred to the stator.

The flux linkage can now be expressed as:

$$\begin{bmatrix} \lambda_{abcs} \\ \lambda'_{abcr} \end{bmatrix} = \begin{bmatrix} L_s & L'_{SR} \\ L'_{RS} & L'_r \end{bmatrix} \times \begin{bmatrix} I_{abcs} \\ I'_{abcr} \end{bmatrix} \quad (31)$$

Equation (31) can be transformed to the arbitrary reference frame as indicated in equation (32) [10].

$$\begin{bmatrix} \lambda_{qdos} \\ \lambda'_{qdor} \end{bmatrix} = \begin{bmatrix} K_s L_s K_s^{-1} & K_s L'_{SR} K_r^{-1} \\ K_r L'_{RS} K_s^{-1} & K_r L'_r K_r^{-1} \end{bmatrix} \times \begin{bmatrix} I_{qdos} \\ I'_{qdor} \end{bmatrix} \quad (32)$$

Where;

$$K_s = \frac{2}{3}\begin{bmatrix} \cos\theta & \cos\left(\theta - \frac{2\pi}{3}\right) & \cos\left(\theta - \frac{4\pi}{3}\right) \\ \sin\theta & \sin\left(\theta - \frac{2\pi}{3}\right) & \sin\left(\theta - \frac{4\pi}{3}\right) \\ \frac{1}{2} & \frac{1}{2} & \frac{1}{2} \end{bmatrix} \quad (33)$$

$$K_s^{-1} = \begin{bmatrix} \cos\theta & \sin\theta & 1 \\ \cos\left(\theta - \frac{2\pi}{3}\right) & \sin\left(\theta - \frac{2\pi}{3}\right) & 1 \\ \cos\left(\theta - \frac{4\pi}{3}\right) & \sin\left(\theta - \frac{4\pi}{3}\right) & 1 \end{bmatrix} \quad (34)$$

$$K_r = \frac{2}{3}\begin{bmatrix} \cos\beta & \cos\left(\beta - \frac{2\pi}{3}\right) & \cos\left(\beta - \frac{4\pi}{3}\right) \\ \sin\beta & \sin\left(\beta - \frac{2\pi}{3}\right) & \sin\left(\beta - \frac{4\pi}{3}\right) \\ \frac{1}{2} & \frac{1}{2} & \frac{1}{2} \end{bmatrix} \quad (35)$$

$$K_s^{-1} = \begin{bmatrix} \cos\beta & \sin\beta & 1 \\ \cos\left(\beta - \frac{2\pi}{3}\right) & \sin\left(\beta - \frac{2\pi}{3}\right) & 1 \\ \cos\left(\beta - \frac{4\pi}{3}\right) & \sin\left(\beta - \frac{4\pi}{3}\right) & 1 \end{bmatrix} \quad (36)$$

Where;

$$\beta = \theta - \theta_r \quad (37)$$

K_s and K_s^{-1} is the transformation and inverse transformation matrix respectively for stator parameters, K_r and K_r^{-1} is the transformation and inverse transformation matrix respectively for rotor parameters.

Evaluating equation (32) with equations (33)-(36) yield the flux linkage in the arbitrary reference frame as shown in equation (38).

$$\begin{bmatrix} \lambda_{qs} \\ \lambda_{ds} \\ \lambda_{os} \\ \lambda'_{qr} \\ \lambda'_{dr} \\ \lambda'_{or} \end{bmatrix} = \begin{bmatrix} L_{ls} + \frac{3}{2}L_{ms} & 0 & 0 & \frac{3}{2}L_{ms} & 0 & 0 \\ 0 & L_{ls} + \frac{3}{2}L_{ms} & 0 & 0 & \frac{3}{2}L_{ms} & 0 \\ 0 & 0 & L_{ls} & 0 & 0 & 0 \\ \frac{3}{2}L_{ms} & 0 & 0 & L'_{lr} + \frac{3}{2}L_{ms} & 0 & 0 \\ 0 & \frac{3}{2}L_{ms} & 0 & 0 & L'_{lr} + \frac{3}{2}L_{ms} & 0 \\ 0 & 0 & 0 & 0 & 0 & L'_{lr} \end{bmatrix} \times \begin{bmatrix} I_{qs} \\ I_{ds} \\ I_{0s} \\ I'_{qr} \\ I'_{dr} \\ I'_{0r} \end{bmatrix} \quad (38)$$

Comparing equation (38) with (28)-(30), it is clear that θ_r has been eliminated from the flux linkage equations by using arbitrary reference frame transformation. It means that the flux linkage is no longer a function of rotor position.

C. Voltage equations in arbitrary reference frame

Taking the stator voltage equations as in equations (1)-(3) and only considering the resistive part, it can be transformed to the arbitrary reference frame as follows:

$$V_{qdos}^{res} = K_s r_s K_s^{-1} I_{qdos} \quad (39)$$

$$K_s r_s K_s^{-1} = \begin{bmatrix} r_s & 0 & 0 \\ 0 & r_s & 0 \\ 0 & 0 & r_s \end{bmatrix} \quad (40)$$

Therefore;

$$V_{qdos}^{res} = r_s I_{qdos} \quad (41)$$

Where;

$$r_s = \begin{bmatrix} r_s & 0 & 0 \\ 0 & r_s & 0 \\ 0 & 0 & r_s \end{bmatrix} \quad (42)$$

The superscript 'res' refers to the resistive part of the voltage equation.
Now considering only the inductive part of the voltage equation as in equations (1)-(3) which can be transformed to the arbitrary reference frame as follows:

$$V_{qdos}^{ind} = K_s \frac{d}{dt}[K_s^{-1}\lambda_{qdos}] \quad (43)$$

Expanding equation (43) using the product rule:

$$V_{qdos}^{ind} = K_s \frac{d}{dt}[K_s^{-1}]\lambda_{qdos} + K_s K_s^{-1}\frac{d}{dt}\lambda_{qdos} \quad (44)$$

Evaluating parts of the terms in equation (44) separately, knowing that;

$$\theta = \int \omega(\xi)d\xi + \theta(0) \quad (45)$$

where ξ is a dummy variable for integration.

$$\frac{d}{dt}[K_s^{-1}] = \omega \begin{bmatrix} -\sin\theta & \cos\theta & 0 \\ -\sin\left(\theta - \frac{2\pi}{3}\right) & -\cos\left(\theta - \frac{2\pi}{3}\right) & 0 \\ -\sin\left(\theta + \frac{2\pi}{3}\right) & -\cos\left(\theta \frac{2\pi}{3}\right) & 0 \end{bmatrix} \quad (46)$$

$$K_s \frac{d}{dt}[K_s^{-1}] = \begin{bmatrix} 0 & \omega & 0 \\ -\omega & 0 & 0 \\ 0 & 0 & 0 \end{bmatrix}$$

$$K_s K_s^{-1} = \begin{bmatrix} 1 & 0 & 0 \\ 0 & 1 & 0 \\ 0 & 0 & 1 \end{bmatrix} \quad (47)$$

Using equations (45)-(47) to evaluate equation (44) yields;

$$V_{qdos}^{ind} = \omega \begin{bmatrix} \lambda_{ds} \\ -\lambda_{qs} \\ 0 \end{bmatrix} + \frac{d}{dt}\begin{bmatrix} \lambda_{qs} \\ \lambda_{ds} \\ \lambda_{os} \end{bmatrix} \quad (48)$$

The superscript 'ind' refers to the inductive part of the voltage equation.
Now adding the voltage equations for the resistive and inductive parts gives the full stator voltage equations in the arbitrary reference frame.

$$V_{qdos} = \begin{bmatrix} r_s & 0 & 0 \\ 0 & r_s & 0 \\ 0 & 0 & r_s \end{bmatrix}\begin{bmatrix} I_{qs} \\ I_{ds} \\ I_{os} \end{bmatrix} + \omega \begin{bmatrix} \lambda_{ds} \\ -\lambda_{qs} \\ 0 \end{bmatrix} + \frac{d}{dt}\begin{bmatrix} \lambda_{qs} \\ \lambda_{ds} \\ \lambda_{os} \end{bmatrix} \quad (49)$$

Using the same method, the rotor voltage equation can be determined.

$$V'_{qdor} = \begin{bmatrix} r'_r & 0 & 0 \\ 0 & r'_r & 0 \\ 0 & 0 & r'_r \end{bmatrix}\begin{bmatrix} I'_{qr} \\ I'_{dr} \\ I'_{or} \end{bmatrix} + (\omega - \omega_r)\begin{bmatrix} \lambda'_{dr} \\ -\lambda'_{qr} \\ 0 \end{bmatrix} + \frac{d}{dt}\begin{bmatrix} \lambda'_{qr} \\ \lambda'_{dr} \\ \lambda'_{or} \end{bmatrix} \quad (50)$$

Where ω, is the rotational speed of the reference frame and ω_r is the rotational speed of the rotor.

The electromagnetic torque in d-q-0 quantities is given as

$$T_e = \left(\frac{3}{2}\right)\left(\frac{P}{2}\right)\left(\lambda_{ds} i_{qs} - \lambda_{qs} i_{ds}\right) \quad (51)$$

Substituting inductances in equation (51) with the expression given in equation (38), equation (52) is achieved as an alternative form of expressing electromagnetic torque in arbitrary reference frame.

$$T_e = \left(\frac{9}{2}\right)\left(\frac{P}{2}\right) L_m\left(i_{dr} i_{qs} - i_{qr} i_{ds}\right) \quad (52)$$

III. SIMULINK IMPLEMENTATION OF INDUCTION MOTOR

MATLAB/Simulink is a tool used to simulate dynamic systems. The Sim Power system is one of the toolboxes in Simulink used to analyze the three-phase induction machine performance under different electrical fault conditions [1]. The dynamic model of three phase induction motor is implemented using MATLAB/Simulink environment as shown in Figure 2. The inputs of a squirrel cage induction motor are the three phase voltages (V_{as}, V_{bs}, V_{cs}), their fundamental frequency and load torque. The outputs are stator currents, rotor currents, electrical torque and rotor speed.

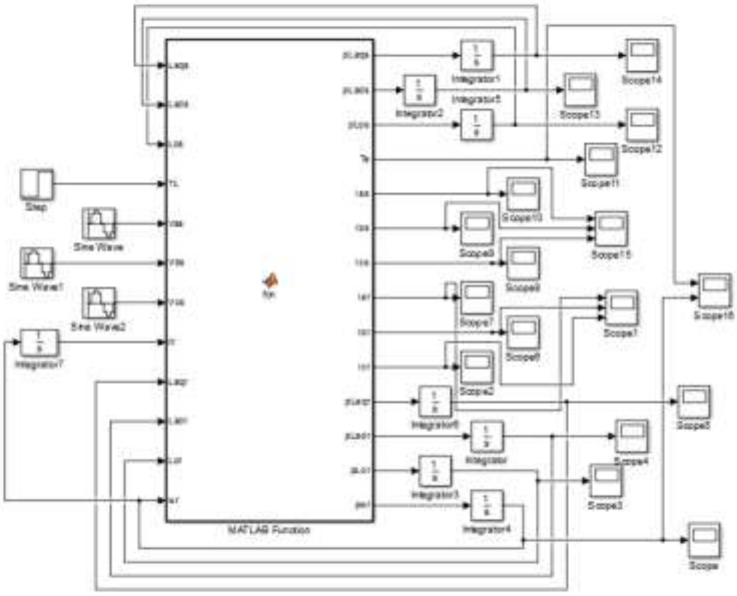

Figure 2: Simulink Block of Induction Motor using Embedded MATLAB Function

IV. SIMULATION RESULTS

The simulation is set to run for a minute. The rated load torque of 14Nm was set to be applied at 1 second when the machine has attained full speed and all the transients had died down. The parameters of 5.5HP motor used for this simulation are shown in Table 1.

Table 1: Machine Parameters

Parameter	Value	Parameter	Value
Rated Voltage	380V	Magnetizing inductance	L_m = 1.1570
Poles	P = 2	Speed	2890rpm
Rated frequency	F = 50	Maximum load	14Nm
Stator winding resistance	R_s = 0.1895		
Rotor winding resistance	R_r = 0.0231		
Stator self-inductance	L_{ls} = 0.1130		
Rotor self-inductance	L_{lr} = 0.1130		

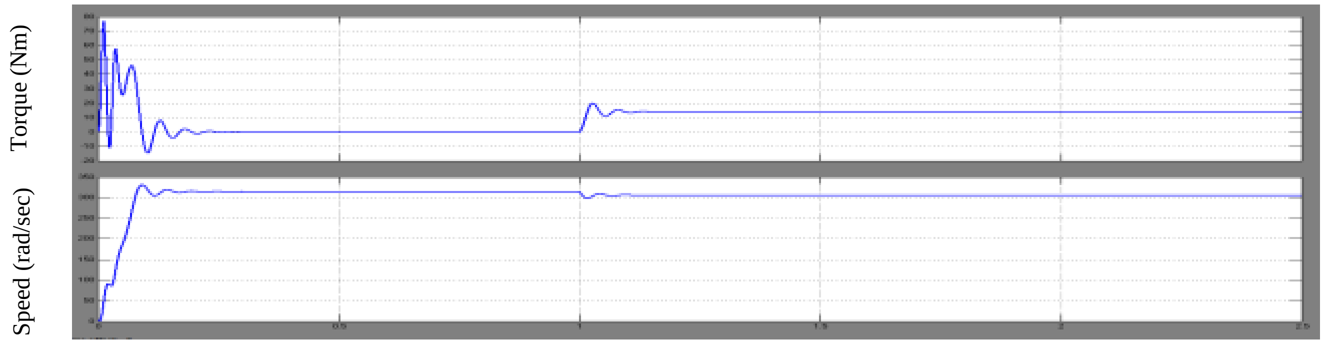

Figure 2: Torque and speed during full rated load (T = 14 Nm)

Figure 2 shows the rotor speed and torque responses with respect to time for the induction motor at full rated load condition. It is seen that prior to the application of the rated load torque, the speed settled at 314 rad/sec (3000 rpm) but on application of rated load, the speed oscillates between 2950 rpm and 2847 rpm before it settled at full load rated speed of 2890 rpm. The torque, in a similar manner, oscillated at the beginning but settled at zero and with the application of full-load after one second, some oscillations were noticed before the torque finally settled down at the rated value.

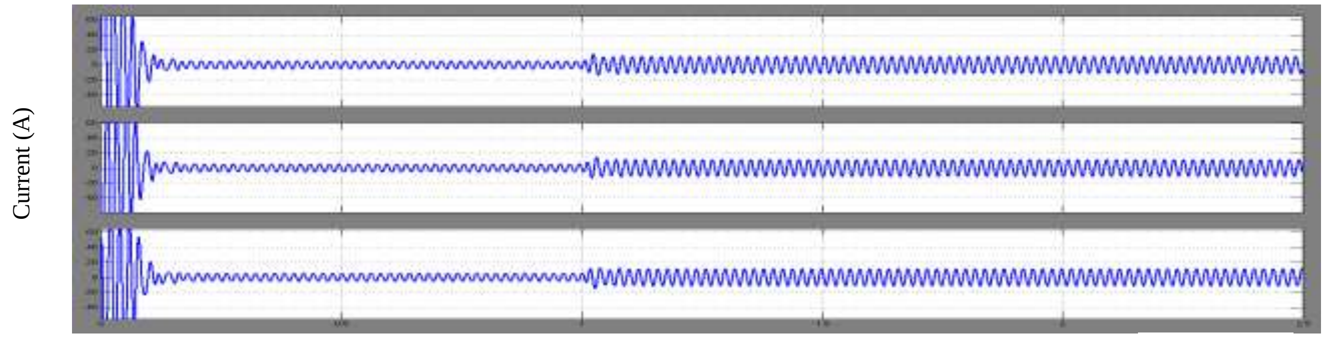

Figure 3: Stator currents during full rated load (T = 14 Nm)

Figure 3 shows the stator currents responses with time. On application of the rated load torque, the currents rose rapidly but again settled at the rated full load current of 9A per phase. Similar current waveforms were observed for the rotor.

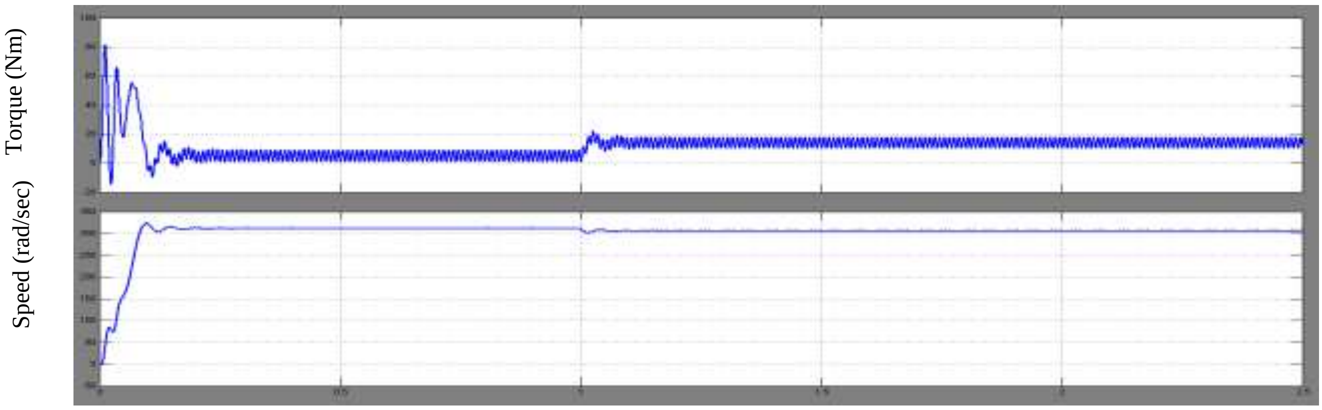

Figure 4: Torque and speed during unbalanced voltage at rated load (T = 14 Nm)

Figure 4 depicts the speed and torque during unbalanced supply voltage at the rated load of 14Nm. Speed ripple and pulsating torque is observed. The speed ripple and fluctuation increased slightly on application of rated load due to uneven distribution of phase currents which could result to vibration of the motor.

International Journal of Modern Trends in Engineering and Research (IJMTER)
Volume: 5, Issue: 05, [May– 2018] **ISSN (Online):2349–9745 ; ISSN (Print):2393-8161**

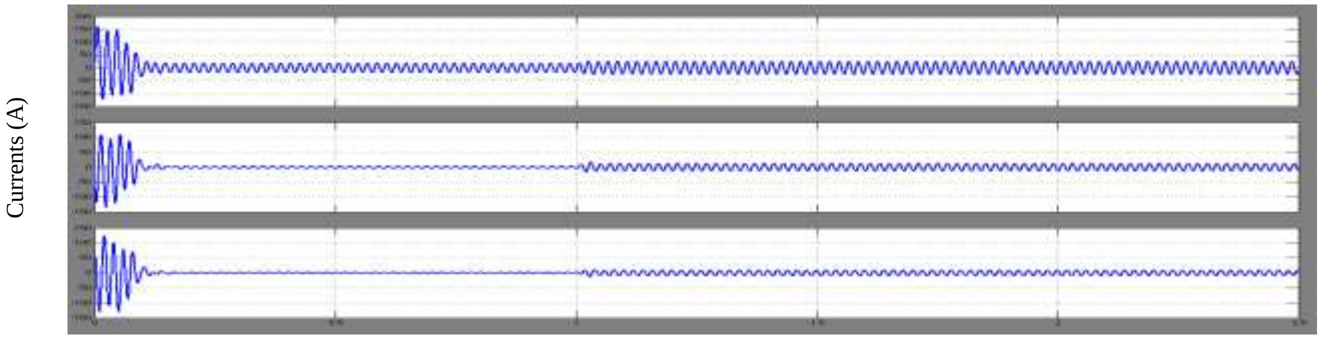

Figure 5: Stator currents during unbalanced voltage at rated load (T = 14Nm)

Figure 5 depicts the stator currents responses with respect to time during unbalanced voltage supply at rated load. Uneven distribution of stator phase currents is seen to be visibly high on application of rated load at one second with phase A having 25A, phase B having 13A and phase C having 9A. These excessive and unbalanced phase currents increase stator losses, reduce the motor efficiency and increase temperature rise, which could damage the windings of the motor.

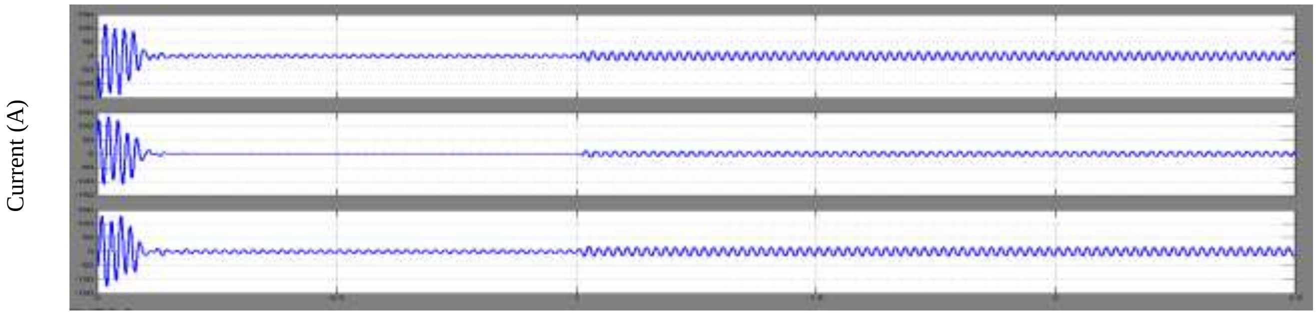

Figure 6: Rotor currents during unbalanced voltage at rated load (T = 14Nm)

Figure 6 depicts the rotor currents increment on application of rated load during unbalanced voltage supply of up to 2 times the rated current at balanced condition.

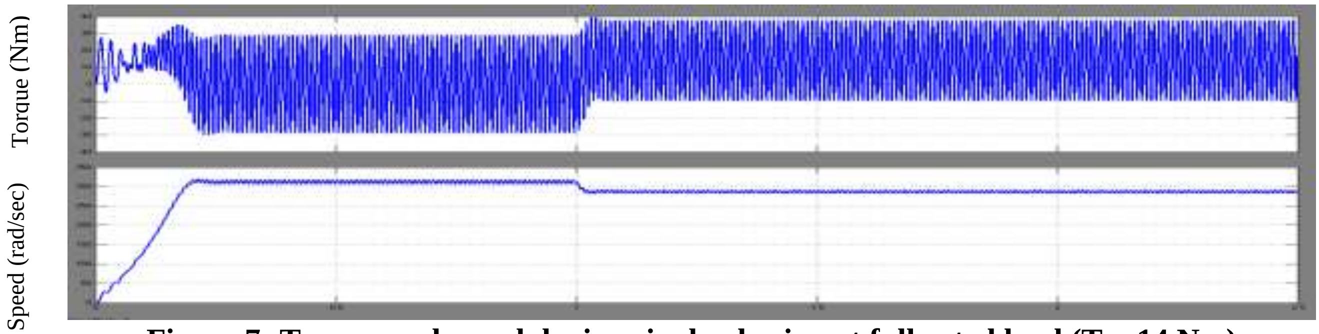

Figure 7: Torque and speed during single phasing at full rated load (T = 14Nm)

Figure 7 is the torque and speed characteristics during single-phasing. It can be noticed that the ripples and oscillations in the torque produced and fluctuations in the speed are seen visibly high compare with the torque and speed produced during voltage unbalanced condition as shown in Figure 5. This implies that single phasing is a worst case of voltage unbalanced.

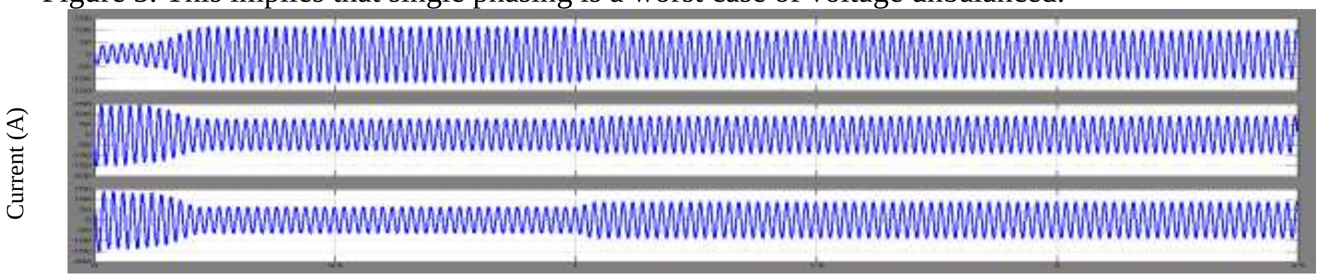

Figure 8: Stator currents during single phasing at full rated load (T = 14Nm)

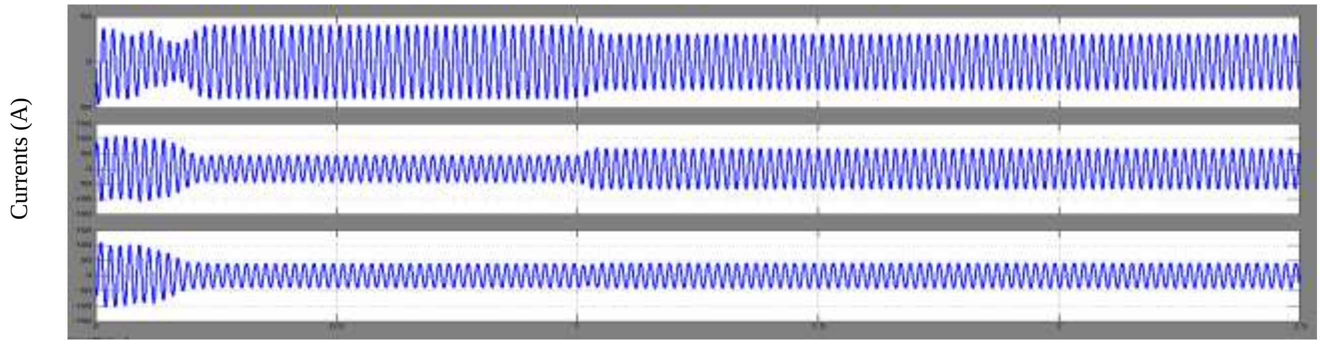

Figure 9: Rotor currents during single phasing at full rated load (T = 14Nm)

From Figure 8 and 9, it is observed that during single phasing; more currents flows through the coil of the cut down phase (Phase A) and more heat will be generated in the stator winding.

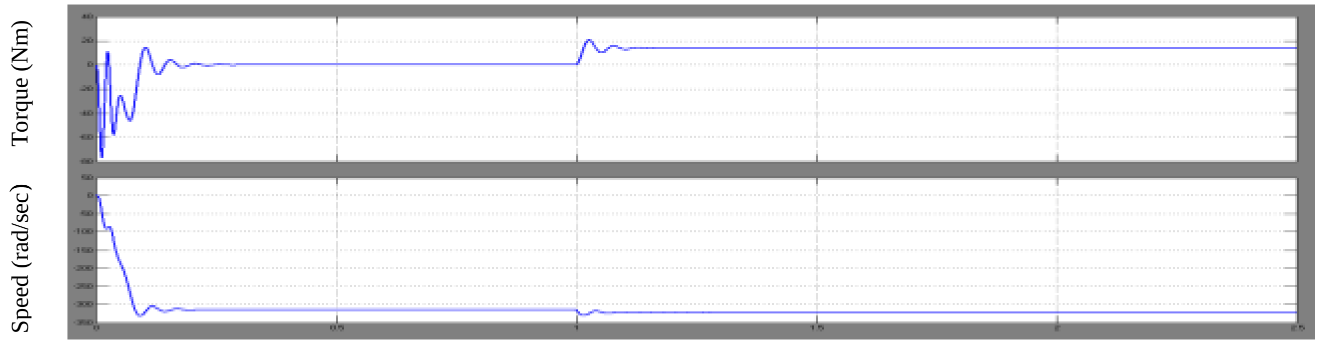

Figure 10: Torque and speed during phase reversal condition at rated load (T = 14 Nm).

From the torque and speed simulation results of phase reversing shown in Figure 10, it is observed that the motor rotates in opposite direction, i.e. the motor runs with negative speed.

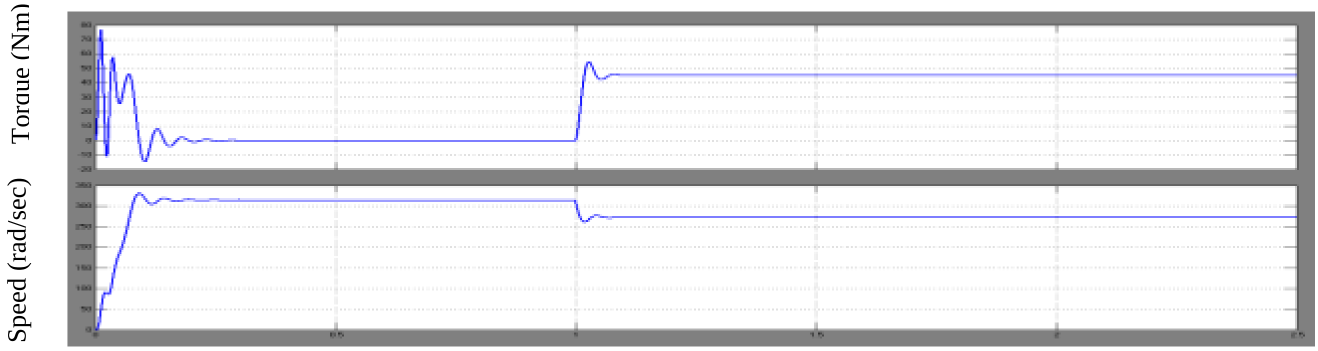

Figure 11: Torque and speed during over load condition (T = 17 Nm).

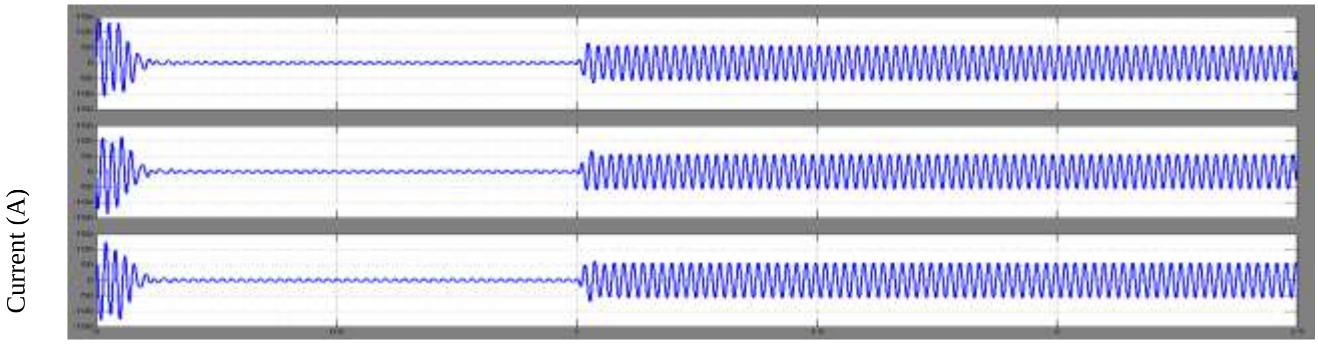

Figure 12: Stator currents during over load condition (T = 17Nm)

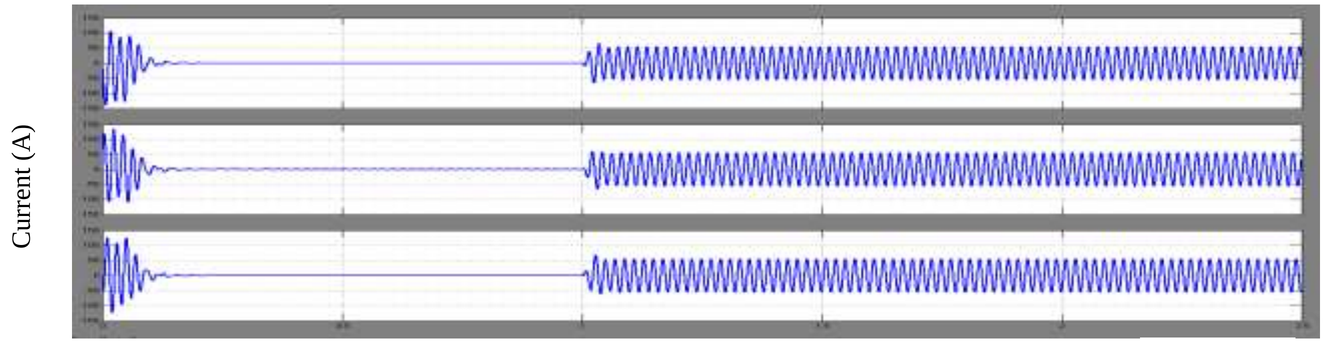

Figure 13: Rotor currents during over load condition (T = 17Nm)

From the simulation results of overload fault condition shown Figure 11, 12 and 13, the following observations are made:

- Increase in phase currents up to a value five times rated current.
- Rapid decrease in the rotor speed to 2599 rpm.
- Harmful effects on machine insulation due to excessive current.

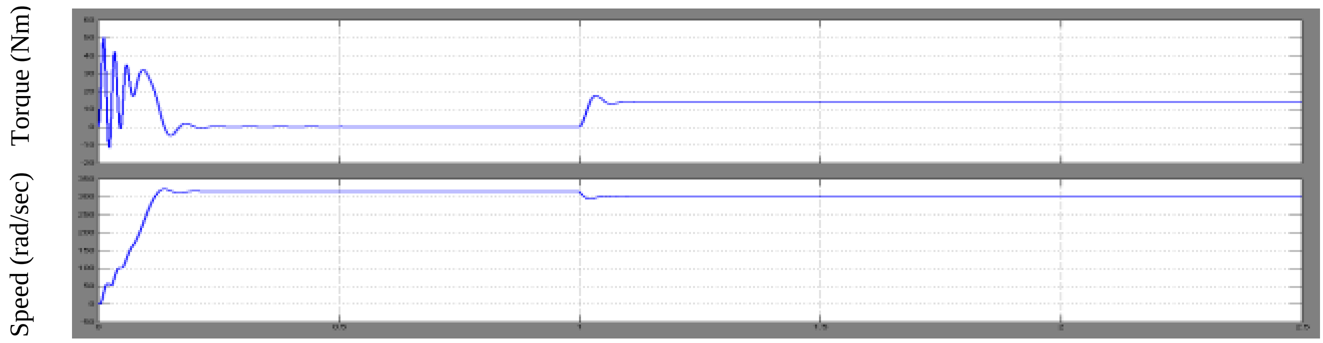

Figure 14: Torque and speed during under voltage condition at full load (T =14Nm)

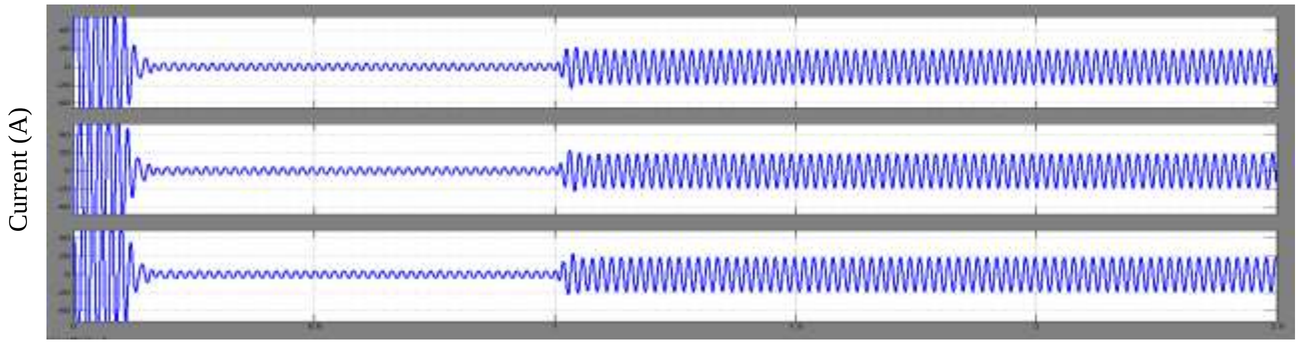

Figure 15: Stator currents during under voltage condition at full load (T = 14Nm)

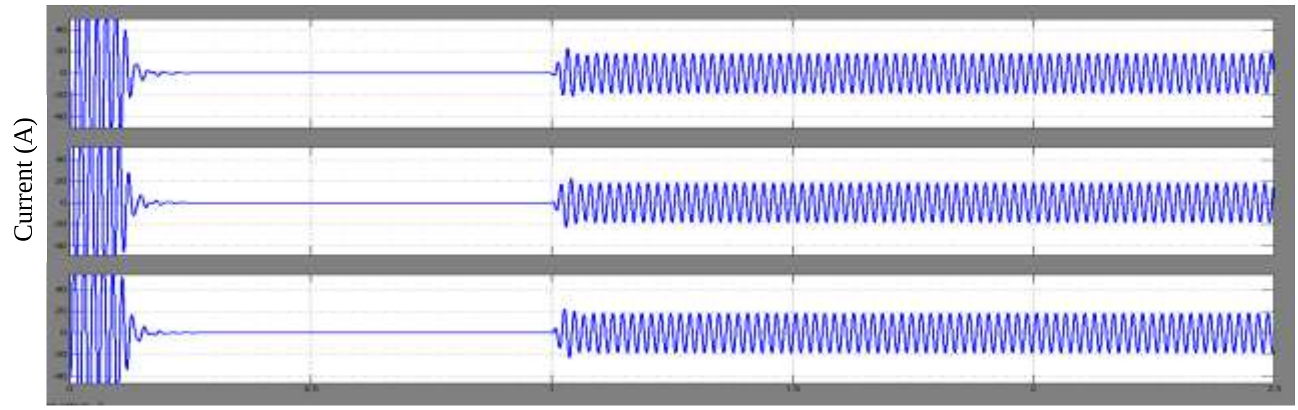

Figure 16: Rotor currents during under voltage condition at full load (T = 14Nm)

From the simulation results of under voltage fault condition shown Figure 14, 15 and 16, the following observations are made:

- It can be seen that the stator and rotor phase currents are twice the rated current.
- There is rapid decrease in rotor speed to a value of 2860 rpm.

V. CONCLUSION

An implementation of the dynamic modeling of various fault conditions of a three-phase induction motor using MATLAB/Simulink is presented in a step-by-step manner. The simulated results in terms of the currents, torque and speed characteristics, are satisfactory [1]-[3]. The model was tested at rated full load condition and different fault conditions. The results show that the MATLAB/Simulink is a reliable and sophisticated software for analysis and prediction of the behavior of induction motor using the reference frames theory.

REFERENCE

[1] M. Sudha and P. Anbalagan, A protection Scheme for three phase Induction Motor from Incipient Faults Using Embedded Controller, Asian Journal of Scientific Research, 2(1), 28-50, 2009.
[2] L.J. Phukon and N. Baruah, A Generalized Matlab Simulink Model of a Three Phase Induction Motor, International Journal of Innovative Research in Science, Engineering and Technology, 4(5): 2926-2934, 2015.
[3] K.L. Shi, T.F. Chan, Y.K. Wong and S.L. Ho, Modeling and Simulation of the Three Phase Induction Motor Using Simulink, International Journal of Engineering Education, 36: 163-172, 1999.
[4] R. Masand, D. Jadwani and S.P. Shukla, Fault Diagnosis of Induction Motor Using PLC, International Journal of Advanced Research in Electrical, Electronics and Instrumentation Engineering, 2(12), 6347-6354, 2013.
[5] K.S. Nithin, B.M. Jos and M. Rafeek, An Improved Method for Starting of Induction Motor with Reduced Transient Torque Pulsations, International Journal of Advanced Research in Electrical, Electronics and Instrumentation Engineering, 2(1), 462-470. 2013.
[6] C. Borse, A. Pandhare and R. Kumar, PLC Based Induction Motor Starting and Protection, International Journal of Engineering Research and General Science, 3(2), 893-897, 2015.
[7] D.R. Sawitri, I.K.E. Purnama and M. Ashari, Detection of Electrical Faults in Induction Motor Fed by Inverter Using Support Vector Machine and Receiver Operating Characteristic, Journal of Theoretical and Applied Information Technology, 40(1), 15-22, 2012.
[8] S. Narwade, P. Kulkarni and C.Y. Patil, Fault Detection of Induction Motor Using Current and Vibration Monitoring, International Journal of Advanced Computer Research, 3(4), 272-279 2013.
[9] A.U. Jawadekar, G.M. Dhole, S.R. Paraskar and M.A. Beg, Novel Wavelet ANN Technique to Classify Bearing Faults in Three phase Induction Motor, 3(3), 48-54, 2011.
[10] T.A. Lipo and D.W. Novotny, Vector Control and Dynamics of AC Drives, In P. Hammond, T.J.E. Miller and T. Kenjo (Eds.), New York, Oxford Science Publications, 1996.
[11] P.C. Krause, Analysis of Electrical Machinery, New York, Macgraw-Hill, 1986.
[12] E.S. Oluwasogo, O.D. Osunde, A.K. Babarinde, I.K.Okakwu, The Dynamic Modelling and Electrical Profile of three phase Induction Motor Using MATLAB Program. Innovative Systems Design and Engineering, 6(1), 38-55, 2015.
[13] S.K. Jain, F. Sharma, M.K. Baliwal, Modelling and Simulation of an Induction Motor, International Journal of Engineering Research and Development, 10(4), 57-61, 2014.